ELSEVIER

Journal of Molecular Catalysis A: Chemical 113 (1996) 479–487

JOURNAL OF MOLECULAR CATALYSIS A: CHEMICAL

Unsupported MoO_3–Fe_2O_3 catalysts: characterization and activity during 2-propanol decomposition

Shar S. Al-Shihry, Samih A. Halawy [*,1]

Department of Chemistry, College of Education, King Faisal University P.O. Box 1759, Al-Hofuf 31982 Eastern Province, Saudi Arabia

Received 5 January 1996; accepted 5 April 1996

Abstract

The catalytic decomposition of 2-propanol (2-PrOH) was studied as probe reaction, in the gas phase, over unsupported MoO_3–Fe_2O_3 mixed catalysts. The samples were prepared by mixing MoO_3 (as ammonium heptamolybdate) with different x mol% Fe_2O_3 (as ferric nitrate) and calcined at 500°C in air for 5 h. All catalysts were characterized by TPR, IR, XRD and XPS analyses. The surface area of these samples were determined using the BET method. Also, the acidity and the basicity of all catalysts were estimated thermogravimetrically using the adsorption of pyridine and formic acid as probe molecules. The catalytic decomposition of 2-PrOH was studied over the catalysts in the temperature range of 150–260°C. A correlation between the catalytic activity and the acidity or the basicity of these catalysts has been made. The activation energies for both propene and acetone formation, over MoO_3–Fe_2O_3 catalysts, were calculated.

Keywords: Acidity; Basicity; Decomposition; Fe_2O_3; IR; MoO_3; 2-propanol; S_{BET}; TPR; XPS; XRD

1. Introduction

MoO_3, Fe_2O_3 and Mo–Fe–O mixed oxides, as pure or supported materials, have emerged as a very important class of catalysts with many areas of industrial applications, such as the oxidation of propene [1], ammonia [2] and butene [3] and thiophene hydrodesulphurization (HDS) [4]. Mixtures of ferrimolybdate and MoO_3 have been widely used in the selective oxidation of methanol to formaldehyde [5,6]. Several techniques have been used to characterize MoO_3 [7,8], Fe_2O_3 [9,10], Fe_2MoO_4 and $Fe_2(MoO_4)_3$ [11–14].

Decomposition of 2-propanol to propene and/or acetone is extensively used to characterize acid–base or redox properties of catalysts [15–18]. The dehydrogenation product (acetone) is preferentially formed on basic catalysts, e.g. Fe_2O_3, while the dehydration product (propene) is essentially formed when acid sites are available [15] as in case of MoO_3 [19]. Recently Ouqour et al. [20] have studied the conversion of 2-propanol, over $CoMoO_4$ and $NiMoO_4$, to investigate the redox and acid–base properties of such catalysts (in presence and absence of air respectively).

The purpose of this work was to characterize the unsupported MoO_3–Fe_2O_3 mixed catalysts,

* Corresponding author.

[1] Permanent address: Chemistry Department, Faculty of Science, South Valley University, Qena 83511, Egypt.

1381-1169/96/$15.00 Copyright © 1996 Elsevier Science B.V. All rights reserved.
PII S1381-1169(96)00155-0

using different techniques, and an attempt has been made to correlate the catalytic activity of these catalysts, during the decomposition of 2-PrOH, with their structure and the acid–base properties.

2. Experimental

2.1. Materials and techniques

Pure MoO_3 and Fe_2O_3 were prepared by calcination of analytical grade ammonium heptamolybdate (AHM) $(NH_4)_6Mo_7O_{24} \cdot 4H_2O$ (Fisons) and ferric nitrate $Fe(NO_3)_3 \cdot 9H_2O$ (Hopkin and Williams) at 500°C for 5 h in air. Samples of MoO_3 containing x mol% Fe_2O_3, after calcination at 500°C (where $x = 0.5$, 5, 10, 30, 50, 70 and 90) were prepared. Calculated amounts of (AHM) and $Fe(NO_3)_3 \cdot 9H_2O$ were used to prepare sufficient amounts of the catalysts as explained previously [19], then the catalyst samples were calcined in air for 5 h at 500°C.

Temperature-programmed reduction (TPR) of the catalysts, calcined at 500°C, was done in apparatus described elsewhere [21]. TPR profiles were recorded at the same experimental conditions as indicated previously [22].

X-ray powder diffraction (XRD) analysis was performed using a Philips diffractometer (P.W. 2103/00) with Ni-filtered CuK_α radiation (λ = 1.542 Å).

IR absorption spectra were recorded by means of a Perkin-Elmer 599B IR spectrophotometer, adopting the KBr disc technique, in the region 1600–200 cm^{-1}.

X-ray photoelectron spectroscopy (XPS) was carried out using a Kratos ES300 spectrometer. The aluminum K_α line (1486.4 eV) was used for excitation. The X-ray power supply was run at 14 kV and 15 mA with a response time of 1 s and a range of 10^{14} CPS.

Surface area measurements were performed using the BET method, using liquid N_2 at −196°C as adsorbate on a Carlo-Erba, single point, SORPTY 1750 unit.

The acidity (Ψ) and the basicity (Φ) of catalyst samples were determined thermogravimetrically, as described previously [23], using the adsorption of pyridine and formic acid as probe molecules. The weight loss was estimated as the acidity or basicity of the catalyst. The values of (Ψ) and (Φ) were calculated [24] as $[H^+]$ or $[OH^-] \times 10^{18}$ ions/m^2 catalyst, respectively.

Measurements of activity and selectivity of all catalysts, during the decomposition course of 2-PrOH, were conducted in a continuous flow system under atmospheric pressure. The detailed experimental procedure is described elsewhere [19]. Also, the reaction rates, catalytic activity, selectivity and the kinetic parameters of the decomposition of 2-PrOH were calculated as explained earlier [19].

3. Results and discussion

3.1. Temperature-programmed reduction (TPR)

The TPR profiles of MoO_3–Fe_2O_3 catalysts calcined, in air, for 5 h at 500°C are shown in Fig. 1. The TPR pattern of MoO_3 (Fig. 1a) displayed two reduction peaks with T_{max} at 683 and 818°C, corresponding to the reduction steps, $MoO_3 \rightarrow MoO_2 \rightarrow Mo$ [25,26], which is confirmed by a ratio of areas under the peaks of approximately (1:2). The experimental H_2 uptake was calculated as 2.14×10^{-2} mol/g (which is in agreement with the theoretical value i.e. 2.08×10^{-2} mol/g). The TPR profile of Fe_2O_3 (Fig. 1i) showed a small peak at 353°C and another big peak at 537°C which might be attributed to stepwise reduction of Fe_2O_3 to metallic Fe [27] as follows:

Fe_2O_3 (hematite) → Fe_3O_4 (magnetite)

→ Fe (metal)

This is in agreement with the reduction mechanism, reported previously [28–30], where

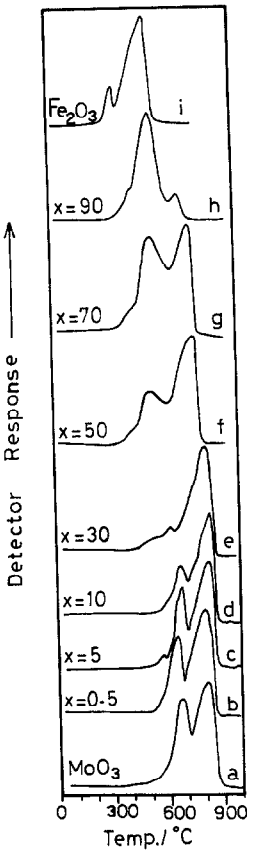

Fig. 1. TPR profiles of MoO_3 (a), MoO_3 mixed with x mol% Fe_2O_3 (b–h) and Fe_2O_3 (i), calcined in air at 500°C for 5 h, carried out at 5°C/min in 6% H_2/N_2 (40 cm^3/min).

no FeO (Wüstite) is encountered below 575°C. Also, this is consistent with the calculated area of the TPR peaks of Fe_2O_3 (Fig. 1i). The hydrogen amount required for the complete reduction of Fe_2O_3 is calculated theoretically [31] as 1.87×10^{-2} mol/g which is in close agreement with the H_2 uptake found (ca. 1.95×10^{-2} mol/g). Evidence for Fe_3O_4 intermediate in reduction of α-Fe_2O_3 has been given, previously, by Gazzarini and Lanzavecchia [32] and Colombo et al. [33].

The addition of 0.5, 5 and 10 mol% Fe_2O_3 to MoO_3 had little effect on the reduction of MoO_3, as the TPR profiles (Fig. 1b–d) have the same reduction peaks as those of MoO_3 with T_{max} shifted to lower values and, in addition, a shoulder at 567–590°C which may be attributed to the reduction of Fe_2O_3. Increasing the mol% Fe_2O_3 added (i.e. 30, 50 and 70 mol% Fe_2O_3) gave different shapes of TPR patterns, (Fig. 1e–g). It is assumed that $Fe_2(MoO_4)_3$ is formed in these samples, containing 30–70 mol% Fe_2O_3, then undergoes a complete reduction to the corresponding Fe and Mo metals in the final stage. These patterns (Fig. 1e–g) are characterized by a shoulder in the range 416–538°C, and a peak at 524–615°C. The shoulder can be due to the reduction of Fe_2O_3 to Fe metal, while the peak located between 524 and 615°C can be related to the reduction of the residual Fe_2O_3, in $Fe_2(MoO_4)_3$, to metallic Fe as well as the reduction of MoO_3 to MoO_2. There is another peak in the temperature range 743–811°C (patterns e–g), which is attributed to the reduction of MoO_2 to Mo metal. It is worth noting here, that significant additions of Fe_2O_3 to MoO_3 (x = 30–70 mol%) have resulted in a catalyzed reduction of MoO_3, to Mo metal, at lower temperatures as reported previously in case of MoO_3–Co_3O_4 system [22,34]. Finally, the TPR profile of MoO_3–90 mol% Fe_2O_3 (Fig. 1h) shows a strong peak at T_{max} = 552°C, with a shoulder at 440°C, corresponds to the reduction of Fe_2O_3 to Fe metal, while the second small one is related to the reduction of MoO_3 to Mo metal at T_{max} = 697°C. The addition of MoO_3 to Fe_2O_3 inhibits the reduction of Fe_2O_3 to Fe metal, because Mo^{6+} ions polarize Fe–O bonds in the same way as Al^{3+} ions do, making them more ionic, and consequently stronger and less reducible [35]. The values of H_2 uptake of MoO_3–Fe_2O_3 catalysts are cited in Table 1. These values increased gradually with the addition of Fe_2O_3 to MoO_3 and attained a maximum (i.e., 2.48×10^{-2} mol/g), at Mo–Fe-V then decreased with increasing Fe_2O_3 content.

3.2. X-ray diffraction analysis

Fig. 2 shows the XRD diffractograms of pure MoO_3 (a), mixed with different x mol% Fe_2O_3 (b–h) and pure Fe_2O_3 (i) calcined at 500°C in

Table 1
Samples description, S_{BET}, acidity–basicity and H_2-uptake of MoO_3–Fe_2O_3 catalysts calcined at 500°C for 5 h in air

Sample description	Mol% oxide at 500°C		$S_{BET}(m^2/g)$	Acidity (Ψ) ($\times 10^{18}$ ions/m^2_{cat})	Basicity (Φ) ($\times 10^{18}$ ions/m^2_{cat})	H_2 uptake ($\times 10^{-2}$ mol/g)
	MoO_3	Fe_2O_3				
MoO_3	100	—	0.8	4.8	—	2.14
Mo–Fe-I	99.5	0.5	0.6	5.1	4.4	2.10
Mo–Fe-II	95.0	5.0	1.8	4.9	5.1	2.30
Mo–Fe-III	90.0	10.0	2.6	4.4	5.9	2.32
Mo–Fe-IV	70.0	30.0	4.2	2.7	6.1	2.39
Mo–Fe-V	50.0	50.0	10.6	2.5	8.3	2.48
Mo–Fe-VI	30.0	70.0	18.3	2.3	8.7	2.13
Mo–Fe-VII	10.0	90.0	29.0	2.0	8.9	2.06
Fe_2O_3	—	100	21.8	1.2	9.5	1.87

air for 5 h. The XRD pattern of Mo–Fe-I (Fig. 2b) had the same characteristic lines of pure MoO_3 (Fig. 2a), especially the main intense lines at $d = 3.818$, 3.466, 3.267, 2.652, 2.309 and 1.852 Å (ASTM card No. 5-0508). The XRD patterns of Mo–Fe-II and Mo–Fe-III (Fig. 2c and d) were characterized by the appearance of a new diffraction line at $d = 3.986$ Å besides the same lines of MoO_3. The intensity of that line increased with increasing Fe_2O_3 content, and became the most intense line in patterns of Mo–Fe-IV and Mo–Fe-V (where $x = 30$ and 50 mol% Fe_2O_3), see Table 1 and Fig. 2 (patterns e and f). This can be due to the formation of the orthorhombic phase of $Fe_2(MoO_4)_3$ [36,37], as it matches well the ferrimolybdate pattern (ASTM card No. 20-526). Our results are in good agreement with previously published work by Chen [38] on iron(III)molybdate, especially those lines at $d = 4.439$, 4.171, 3.969, 3.520,

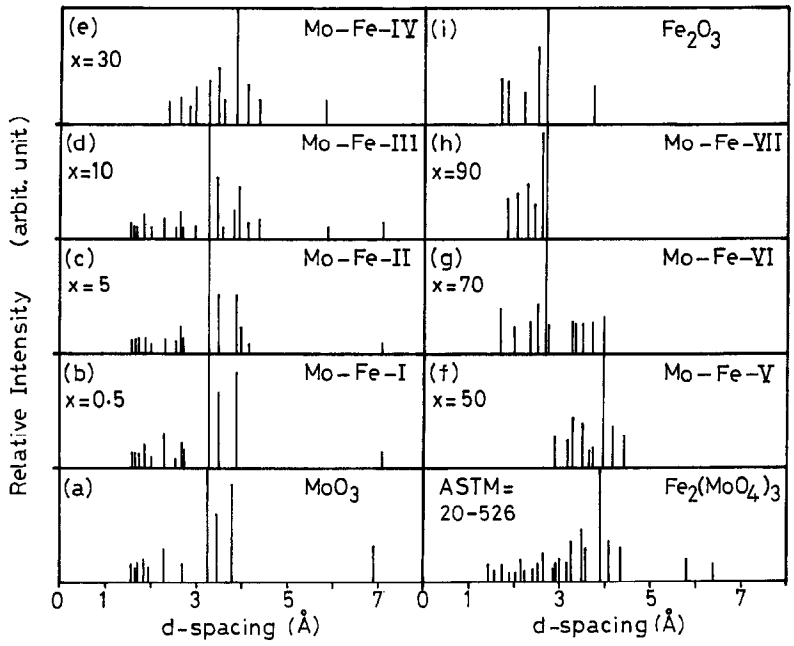

Fig. 2. XRD patterns of MoO_3 (a), MoO_3 mixed with x mol% Fe_2O_3 (b–h) and Fe_2O_3 (i), calcined in air at 500°C for 5 h.

3.290 and 2.885 Å. The XRD diffractogram of Mo–Fe-VI showed an observed decrease in the intensity of the diffraction line assigned to $Fe_2(MoO_4)_3$ at $d = 3.986$ Å, which has completely vanished from pattern (h) of Mo–Fe-VII (containing 90 mol% Fe_2O_3). There is a new diffraction line appearing in patterns (Fig. 2g and h) of Mo–Fe-VI and Mo–Fe-VII at $d = 2.730$ Å with $I/I^\circ = 100$, which is ascribed to the separation of Fe_2O_3 in these mixtures. The XRD pattern of Mo–Fe-VII is almost identical with the pattern of pure Fe_2O_3 (ASTM card No. 24-27A, see also (Fig. 2i), where the diffraction lines are at $d = 3.728$, 2.704, 2.515, 2.206 and 1.692 Å.

From the XRD analysis, one can notice that the formation of $Fe_2(MoO_4)_3$ has started in sample (Mo–Fe-II) containing 5 mol% Fe_2O_3, while samples Mo–Fe-IV and Mo–Fe-V (containing 30 and 50 mol% Fe_2O_3) showed the maximum concentration of ferrimolybdate formed among these mixtures, as suggested from TPR analysis. Increasing the Fe_2O_3 content up to 90 mol% in these mixtures gave identical XRD pattern of Fe_2O_3.

3.3. IR analysis

From the recorded spectra of MoO_3–Fe_2O_3 catalysts calcined at 500°C the spectra of MoO_3, Mo–Fe-I, Mo–Fe-II and Mo–Fe-III (Fig. 3a–d) have the same absorption band at 990 cm^{-1}, which can be due to Mo = O stretching mode [38], followed by a group of bands in the range 850–555 cm^{-1} which are attributed to the stretching mode of the bridge oxygen Mo–O–Mo [39]. Also, the bands of the deformation mode of O–Mo–O in the region 420–230 cm^{-1} appear in these spectra (Fig. 3a–d). The IR spectra of samples Mo–Fe-IV, Mo–Fe-V and Mo–Fe-VI (containing 30, 50 and 70 mol% Fe_2O_3) showed new bands at 855–840 cm^{-1} and 550–535 cm^{-1}, which are related to the formation of $Fe_2(MoO_4)_3$ in these mixtures and assigned to ν(Fe–Mo–O) [40–42] as well as the frequencies assigned to O–Mo–O. The observed frequencies of IR spectra of such samples (Fig. 3e–g) are consistent with those reported by Cord et al. [43]. The IR spectrum of Fe_2O_3 (Fig. 3i) showed the characteristic frequencies of α-Fe_2O_3 (hematite) [44] at 560, 470, 380 and 395 cm^{-1}. Finally, the spectrum of Mo–Fe-VII (see Table 1) showed the similar bands of α-Fe_2O_3 besides a group of absorption bands at 665 and 445–225 cm^{-1} due to O–Mo–O deformation mode.

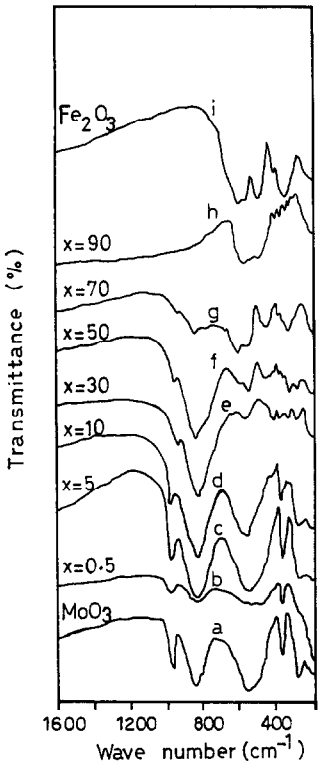

Fig. 3. IR spectra of MoO_3 (a), MoO_3 mixed with x mol% Fe_2O_3 (b–h) and Fe_2O_3 (i), calcined in air at 500°C for 5 h.

The IR results support the XRD results, where $Fe_2(MoO_4)_3$ is clearly shown to be formed by the IR spectrum and XRD pattern of Mo–Fe-V (containing 50 mol% Fe_2O_3) and Mo^{6+} ions are characterized in all spectra (Fig. 3), except for spectra (h) and (i), by two absorption bands at 960 and 840 cm^{-1} [45].

3.4. XPS results

The values of the binding energies of Mo 3d and Fe 2p levels for MoO_3–Fe_2O_3 catalysts,

Table 2
Binding energies (±0.5 eV) relative to C 1s = 284.6 eV of Mo 3d and Fe 2p levels for MoO_3–Fe_2O_3 catalysts, calcined at 500°C for 5 h in air

Sample	Mo		Fe	
	$3d_{5/2}$	$3d_{3/2}$	$2p_{3/2}$	$2p_{1/2}$
MoO_3	233.4	236.5	—	—
Mo–Fe-I	233.4	236.5	712.4	726.0
Mo–Fe-II	230.7	233.5	711.8	725.4
Mo–Fe-III	229.7	233.0	710.6	724.6
Mo–Fe-IV	230.7	233.0	710.1	724.4
Mo–Fe-V	230.3	233.2	712.6	727.6
Mo–Fe-VI	230.2	233.1	712.5	727.2
Mo–Fe-VII	230.2	233.2	713.4	725.6
Fe_2O_3	—	—	713.6	727.2

under investigation, are listed in Table 2. All binding energies were referenced to the contaminated carbon (C 1s = 284.6 eV). The binding energy of the Mo $3d_{5/2}$ level was 233.4 eV, in case of MoO_3 and Mo–Fe-I, indicating the presence of higher Mo–O oxidation states which are characteristic of Mo^{6+} [12,46]. The addition of x mol% Fe_2O_3 (i.e. $x = 5$, 10, 30, 50, 70, and 90) has lowered the binding energy of Mo 3d level from 233.4 to about 230.0 eV. This new value indicated the presence of Mo^{5+} and Mo^{6+} in these mixtures, as reported by Patterson et al. [47] in MoO_3/Al_2O_3 reduced catalysts.

In case of Fe_2O_3, the binding energies of Fe $2p_{3/2}$ and Fe $2p_{1/2}$ levels were calculated as 713.6 and 727.2 eV respectively. These values match those published by Armour et al. [48]. The binding energy of Fe $2p_{3/2}$ level (ca. 713.6 eV) corresponds to Fe^{3+} [49]. The addition of MoO_3 to Fe_2O_3 has slightly changed the binding energy of Fe $2p_{3/2}$ and Fe $2p_{1/2}$ to lower values, see Table 2. Our results are consistent with those obtained by other workers [50,51] for Fe_2O_3–MoO_3 catalysts.

3.5. Catalytic activity measurements

The effect of catalyst composition of MoO_3–Fe_2O_3 system, calcined at 500°C for 5 h in air, on the decomposition of 2-PrOH at 200°C are shown in Fig. 4. The activity of MoO_3 is greatly affected by the addition of 0.5 mol% Fe_2O_3,

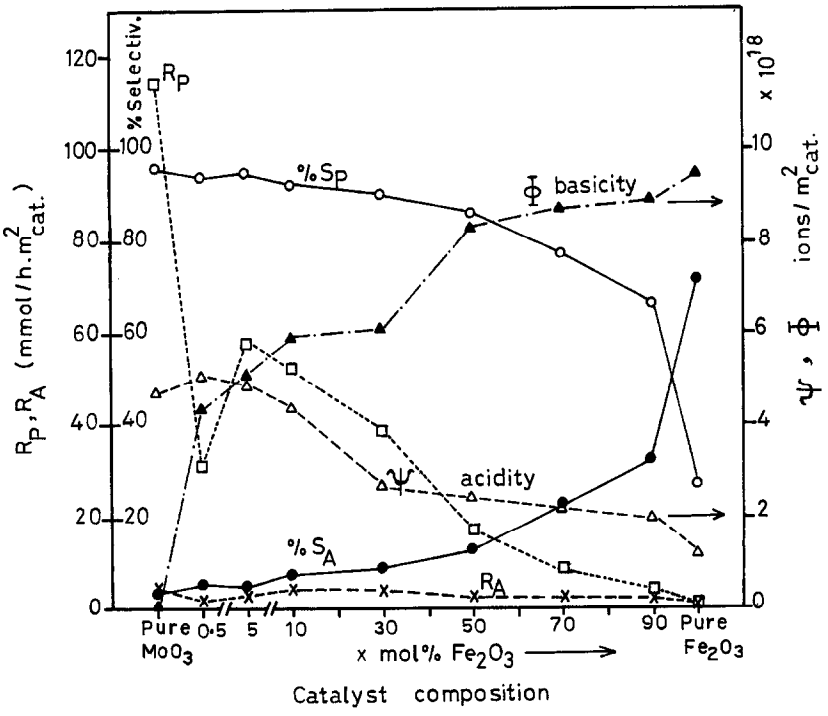

Fig. 4. Effect of catalyst composition on its acidic–basic properties and activity, during the decomposition of 2-propanol, of MoO_3–Fe_2O_3 catalysts calcined in air at 500°C for 5 h.

where R_p (the rate of propene formation) decreased to about one quarter of its original value for MoO_3. Increasing Fe_2O_3 content to 5 mol% Fe_2O_3 improved the value of R_p to 57.8 mmol/h · m^2_{cat}, then it decreased gradually with increasing the mol% Fe_2O_3. MoO_3 is mainly selective towards propene formation but a continuous increase in mol% Fe_2O_3 added to MoO_3 results in a notable decrease in % S_p (% propene selectivity), see Fig. 4. The lessening of % S_p goes parallel with the decrease in the measured values of the acidity (Ψ) of these catalysts, see Table 1. Fe_2O_3 is highly selective towards acetone formation (i.e. % $S_a = 72.3$), with a relatively lower value of propene selectivity (i.e. % $S_p = 27.7$). The calculated values of R_a (the rate of acetone formation) of MoO_3–Fe_2O_3 system, Fig. 4 and Table 3, were very small related to the values of R_p of these catalysts. This is because the basic sites on Fe_2O_3, that are responsible for the formation of acetone [15], were still inactive at 200°C where the dehydrogenation of 2-PrOH was carried out, as in case of the selective oxidation of butene [3]. The gradual increase of % S_a with increasing the amount of Fe_2O_3 in the catalysts, also, goes parallel with the measured values of the basicity (Φ) of such samples, see Fig. 4 and Table 1.

The % conversion over Mo–Fe-I is nearly one fifth of its value over MoO_3. Also, % conversion increased gradually with increasing mol% Fe_2O_3 added to MoO_3. The maximum value of % conversion (ca. 38.3%) is located at sample Mo–Fe-V, containing 50 mol% Fe_2O_3. The addition of 70 and 90 mol% Fe_2O_3 to MoO_3 decreased gradually % conversion of 2-PrOH over such samples. Fe_2O_3, on the other hand, has a very low activity towards 2-PrOH decomposition at the same experimental conditions (% conversion = 2.4%).

The dehydration reaction of 2-PrOH is catalyzed at acidic sites and the dehydrogenation reaction is catalyzed at both acidic and basic sites [52]. MoO_3 has Brönsted acidity [53] and its measured acidity (Ψ) = 4.8×10^{18} ions/m^2_{cat}, therefore it is mainly selective towards propene formation. Fe_2O_3, on the other hand, has Brönsted basicity ($\Phi = 9.5 \times 10^{18}$ ions/m^2_{cat}) with the presence of some acid sites [54] ($\Psi = 1.2 \times 10^{18}$ ions/m^2_{cat}), and consequently Fe_2O_3 is selective towards both acetone and propene formation (see Table 3). The addition of Fe_2O_3 to MoO_3 has resulted in a gradual increase in its activity, due to the generation of new sites $V_{Mo^{6+}}$ (molybdenum vacancies) and $V_{O^{2-}}$ (oxygen vacancies) during the formation of $Fe_2(MoO_4)_3$ according to the equation [36]:

$$3MoO_3 + Fe_2O_3 \rightarrow Fe_2(MoO_4)_3 + V_{Mo^{6+}} + 3V_{O^{2-}}$$

Increasing the concentration of $Fe_2(MoO_4)_3$, in these mixtures, leads to the generation of

Table 3
Kinetic parameters for the decomposition of 2-PrOH over MoO_3–Fe_2O_3 catalysts, calcined at 500°C for 5 h in air as well as the activation energies for propene and acetone formation at the corresponding temperature ranges

Catalyst description	% conversion	$R_{2\text{-PrOH}}$ (mmol/h · m^2_{cat})	R_p (mmol/h · m^2_{cat})	R_a (mmol/h · m^2_{cat})	Temperature range (°C)	E_p (kJ/mol)	E_a (kJ/mol)
MoO_3	17.7	118.2	113.8	4.4	180–210	75 ± 5	46 ± 8
Mo–Fe-I	3.7	33.0	31.2	1.8	200–250	67 ± 6	53 ± 10
Mo–Fe-II	20.4	60.8	57.8	3.0	160–200	102 ± 5	71 ± 3
Mo–Fe-III	27.5	56.7	52.0	4.7	150–200	109 ± 7	59 ± 6
Mo–Fe-IV	32.8	41.8	37.8	4.0	150–200	106 ± 8	58 ± 3
Mo–Fe-V	38.3	19.3	16.8	2.5	150–185	103 ± 4	65 ± 2
Mo–Fe-VI	36.2	10.6	8.2	2.4	150–200	101 ± 6	63 ± 9
Mo–Fe-VII	35.1	6.5	4.3	2.2	150–200	99 ± 2	75 ± 7
Fe_2O_3	2.4	0.6	0.2	0.4	220–260	110 ± 3	130 ± 8

$R_{2\text{-PrOH}}$ = total rate of removal of 2-PrOH; % reactant = 1.2%; $W/F = 1.87$ g cat mol/L · h; total flow rate = 100 mL/min; reaction temperature = 200°C.

more cation–anion pair sites in the catalysts. Sample Mo–Fe-V, containing 50 mol% Fe_2O_3, showed the maximum concentration of $Fe_2(MoO_4)_3$, as confirmed by XRD and IR analyses (see Figs. 2 and 3); then $Fe_2(MoO_4)_3$ diminished gradually in samples containing > 50 mol% Fe_2O_3. This is consistent with the above equation and the experimental data (Table 3 and Fig. 4). Also, % S_p decreased gradually due to the replacement of Mo^{6+} by Fe^{3+} in these mixtures and consequently the expected yield of the dehydration reaction of 2-PrOH will decrease [36]:

$$C_3H_7OH + Mo^{6+} + O^{2-} \rightarrow Mo^{5+} + CH_3{-}CH{=}CH_2 + H_2O$$

The activation energy for propene and acetone formation (E_p and E_a) was calculated from the Arrhenius plots of log R_p (rate of propene formation) or log R_a (rate of acetone formation) against $1/T$ as explained previously [19]. The values of E_p increased gradually from 67 ± 6 to 99 ± 2 kJ/mol with increasing mol% Fe_2O_3 in these mixtures and, also, with decreasing the acidity of the catalysts, see Tables 1 and 3. The values of E_a is ranging between 53 ± 10 and 75 ± 7 kJ/mol for the mixed catalysts. The calculated values of E_p and E_a in this work, are in great agreement with those published recently, on $CoMoO_4$ and $NiMoO_4$, by Ouqour et al. [20]. From the values of E_p and E_a of pure Fe_2O_3 (Table 3) one can notice that the higher values of the activation energy (and low % conversion) suggests that Fe_2O_3 is still an inactive catalyst at the applied range of temperature (220–260°C) compared with other catalysts in this series. Fe_2O_3 is known to be a very active catalyst at higher temperatures (> 350°C) as in case of the selective oxidation of butene to butadiene [3].

4. Conclusions

Finally, it is concluded that the decomposition of 2-PrOH over MoO_3–Fe_2O_3 catalysts, calcined at 500°C for 5 h in air, depends mainly on two factors: (i) the composition of the catalysts, where the sample with the composition of (MoO_3–50 mol% Fe_2O_3) in this series was shown to be the most active one. It contains the highest concentration of $Fe_2(MoO_4)_3$, accompanied by the generation of more cation–anion pair sites, as confirmed by XRD and IR analyses; and (ii) the surface acidic–basic characters of these catalysts. The addition of increased amounts of Fe_2O_3 (as mol%) to MoO_3 have resulted in a continuous decrease of the concentration of Brönsted acidic sites and, consequently, an increase in the concentration of the basic Brönsted sites on their surfaces. This is parallel with the increments of (% S_a) selectivities of the catalysts towards acetone production.

Acknowledgements

We gratefully acknowledge Professor G.C. Bond and the staff of his laboratory, Department of Chemistry, Brunul University, UK, for their valuable help in TPR measurements.

References

[1] B. Benaichouba, P. Bussiere and J.C. Vedrine, Appl. Catal. A: Gen. 130 (1995) 31.
[2] J.J.P. Biermann, F.J.J.G. Janssen, M. de Boer, A.J. Van Dillen, J.W. Geus and E.T.C. Vogt, J. Mol. Catal. 60 (1990) 229.
[3] B.L. Yang, F. Hong and H.H. Kung, J. Phys. Chem. 88 (1984) 2531.
[4] J.M. Lewis and R.A. Kydd, J. Catal. 136 (1992) 478.
[5] Y. Matsuoka, M. Niwa and Y. Murakami, J. Phys. Chem. 94 (1990) 1477.
[6] C.J. Machiels, W.H. Cheng, U. Chowdhry, W.E. Farneth, F. Hong, E.M. McCarron and A.W. Sleight, Appl. Catal. 25 (1986) 249.
[7] S. Rajagopal, H.J. Marini, J.A. Marzari and R. Miranda, J. Catal. 147 (1994) 417.
[8] P.A. Spevack and N.S. McIntyre, J. Phys. Chem. 96 (1992) 9029.
[9] S.A. Halawy and M.A. Mohamed, Collect. Czech. Chem. Commun. 59 (1994) 2253.

[10] P.A. Chernavskii, V.V. Kiselev and V.V. Lunin, Zh. Fiz. Khim. 66 (1992) 2717.
[11] M.M. Gasik and P.N. Ostrik, J. Therm. Anal. 40 (1993) 313.
[12] B. Domenichini, B. Gillot and P. Tailhades, Thermochim. Acta 205 (1992) 259.
[13] M. Karroua, J. Ladrière, H. Matralis, P. Grange and B. Delmon, J. Catal. 138 (1992) 640.
[14] Y.L. Xiong, R. Castillo, Ch. Papadopoulou, L. Daza, J. Ladrière, P. Ruiz and B. Delmon, Catalyst Deactivation, C.H. Bartholomew and J.B. Butt (Eds.) (Elsevier, Amsterdam, 1991) p. 425.
[15] J.M. Campelo, A. Garcia, J.F. Herencia, D. Luna, J.M. Marinas and A.A. Romero, J. Catal. 151 (1995) 307.
[16] S.A. Halawy, M.A. Mohamed and S.F. Abd El-Hafez, J. Mol. Catal. 94 (1994) 191.
[17] F. Pepe, C. Angeletti and S. De Rossi, J. Catal. 118 (1989) 1.
[18] H. Pines, in: The Chemistry of Catalyic Hydrocarbon Conversions (Academic Press, New York, 1981) p. 127.
[19] G.C. Bond, S.A. Halawy, K.M. Abd El-Salaam, E.A. Hassan and H.M. Ragih, J. Chem. Technol. Biotechnol. 59 (1994) 181.
[20] A. Ouqour, G. Coudurier and J.C. Vedrine, J. Chem. Soc. Faraday Trans. 89 (1993) 3151.
[21] S. Flamerz, Ph.D. thesis, Brunel University, U.K., 1988.
[22] S.A. Halawy, M.A. Mohamed and G.C. Bond, J. Chem. Technol. Biotechnol. 58 (1993) 237.
[23] S.A. Halawy and M.A. Mohamed, J. Mol. Catal. A: Chem. 98 (1995) 63.
[24] M.A. Makarova, E.A. Paukshtis, J.M. Thomas, C. Williams and K.I. Zamaraev, J. Catal. 149 (1994) 36.
[25] J. Brito, J. Laine and K.C. Pratt, J. Mater. Sci. 24 (1989) 425.
[26] P. Arnoldy, J.C.M. de Jonge and J.A. Moulijn, J. Phys. Chem. 89 (1985) 4517.
[27] E.E. Unmuth, L.H. Schwartz and J.B. Butt, J. Catal. 63 (1980) 404.
[28] M. Shimokawabe, R. Furuichi and T. Ishii, Thermochim. Acta 28 (1979) 287.
[29] J. Bessières and J.J. Heizmann, Int. J. Hydrogen Energy, 5 (1980) 585.
[30] M.V.C. Sastri, R.P. Viswanath and B. Viswanathan, Int. J. Hydrogen Energy 7 (1982) 951.
[31] R. Brown, M.E. Cooper and D.A. Whan, Appl. Catal. 3 (1982) 177.
[32] F. Gazzarini and G. Lanzavecchia, Proc. 6th Int. Symp. on Reactivity of Solids, Schenectady, NY, August 1968.
[33] Y. Colombo, F. Gazzarini and G. Lanzavecchia, Mater. Sci. Eng. 2 (1967) 125.
[34] J.M. Zabala, P. Grange and B. Delmon, CR Acad. Sci. Paris C 561 (1974) 279.
[35] P. Arnoldy and J.A. Moulijn, J. Catal. 93 (1985) 38.
[36] A.A. Said, Bull. Chem. Soc. Jpn. 65 (1992) 3450.
[37] V. Massarotti, G. Flor and A. Marini, J. Appl. Cryst. 14 (1981) 64.
[38] M. Niwa, M. Kizutani, M. Takahashi and Y. Murakami, J. Catal. 70 (1981) 14.
[39] F. Trifiro, S. Notarbartolo and I. Pasquon, J. Catal. 22 (1971) 324.
[40] P. Forzatti, P.L. Villa, N. Ferlazzo and D. Jones, J. Catal. 76 (1982) 188.
[41] P.L. Villa, A. Szabo, F. Trifiro and M. Carbucicchio, J. Catal. 47 (1977) 122.
[42] T.S.R. Prasada Rao and K.R. Krishnamurthy, J. Catal. 95 (1985) 209.
[43] P.P. Cord, P. Courtine, G. Pannetier and J. Guillermet, Spectrochim. Acta A 28 (1972) 1601.
[44] N.T. McDevitt and W.L. Baun, Spectrochim. Acta 20 (1964) 799.
[45] B. Gillot, B. Domenichini, Ph. Tailhades, L. Bouet and A. Rousset, Solid State Ionics 63–65 (1993) 620.
[46] Y. Okamoto, K. Oh-Hiraki, T. Imanaka and S. Teranishi, J. Catal. 71 (1981) 99.
[47] T.A. Patterson, J.C. Carver, D.E. Leyden and D.M. Hercules, J. Phys. Chem. 80 (1976) 1700.
[48] A.W. Armour, P.C.H. Mitchell, B. Folkesson and R.J. Larrsson, Less-Common. Met. 36 (1974) 361.
[49] C.R. Brundle, T.J. Chuang and K. Wandelt, Surf. Sci. 68 (1977) 459.
[50] B.I. Popov, A.V. Pashis and L.N. Shkuratova, React. Kinet. Catal. Lett. 30 (1986) 129.
[51] Y. Okamoto, F. Morikawa, K. Oh-Hiraki, T. Imanaka and S. Teranishi, J. Chem. Soc. Chem. Commun. (1981) 1018.
[52] M. Ai, J. Catal. 50 (1977) 291.
[53] T. Fransen, O. Van der Meer and P. Mars, J. Phys. Chem. 80 (1976) 2103.
[54] C.P. Bezouhanova and M.A. Al-Zihari, Catal. Lett. 11 (1991) 245.